Stress transmission in silica particulate epoxy composite by X-ray diffraction*

Ai-Ru Xu, Takashi Nishino and Katsuhiko Nakamae†
Department of Industrial Chemistry, Faculty of Engineering, Kobe University, Rokkodai-cho, Nada, Kobe 657, Japan
(Received 10 January 1992; revised 16 March 1992; accepted 7 April 1992)

Stress on particles in silica particulate epoxy composite under constant load was investigated by X-ray diffraction. Microdeformation of the crystal lattice of silica could be detected as a shift of the X-ray diffraction peak induced by the applied stress. When a tensile stress was applied to the particulate composite, incorporated particles were found to be subjected to a stress several times larger than the applied stress. The stress concentration onto particles in particulate composite material, which was considered to result in a mechanical reinforcement of the composite, depends on the volume fraction and size of particles. Quantitative relationships between the stress concentration coefficient, particle diameters and the increment of macroscopic Young's modulus with the incorporation of filler were stated.

(Keywords: stress transmission; particulate composite material; X-ray diffraction; epoxy resin; stress concentration; mechanical property)

INTRODUCTION

Materials consisting of more than two kinds of substance, that is, composite materials, have been designed for complying with various demands. Plastics, paints and rubbers incorporating powdery fillers have frequently been used from the view point of mechanical properties. For these particulate composite materials, it is important to clarify the reinforcement effect of fillers. A variety of theoretical and experimental studies have been reported on the reinforcement effect in terms of macroscopic mechanical properties[1,2]. However, there are a lot of difficulties because of uncertainty in adhesion between matrix and fillers, complex deformation in the composite and so on. In order to investigate the factors which influence the mechanical properties, we proposed a new technique, the 'X-ray diffraction method', to detect the residual stress at the interface between resin and adherend[3,4]. By using this method, microdeformation of the adherend crystal can be detected as a shift of the X-ray diffraction peak induced by the residual stress. Results show that the adherend is subjected to a uniaxial compressive stress parallel to the adherend surface. In contrast to this, the epoxy resin side was found to be subjected to a uniaxial tensile stress by obeying the law of action and reaction[3,4]. This X-ray diffraction method is also utilized to detect the stress concentrated onto particles in Al particulate epoxy composite, and the reinforcement effect of fillers was discussed by using a 'stress concentration coefficient' in the previous paper[5]. It was found that particles in eopxy composite were subjected to a tensile stress several times larger than the applied stress when the composite was under load. In this study, stress on particles in the silica particulate composite under tensile load was measured *in situ* by using X-ray diffraction; the reinforcement behaviour and the difference in stress concentration coefficients of particulate composites incorporating different silica particle sizes were discussed from the microscopic point of view.

EXPERIMENTAL

Specimen preparation

A liquid diglycidyl ether of bisphenol A type epoxy resin (Epikote 828; Shell Chemical Co.; $M_n = 380$, epoxy equivalent 190 ± 5, $n = 0.1$) (*Structure 1*) and 4,4'-diaminodiphenylmethane (DDM), an aromatic diamine curing agent (*Structure 2*) were chosen as the resin system in this study. The fillers used were air blown fractionated silica (α-quartz, Tatsumori Co.) particles with average diameters of 1.5 μm, 6.2 μm and 27 μm.

Figure 1 shows the scanning electron microphotographs (Hitachi S-2500, accelerating voltage 10 kV) of these three kinds of silica particle. As usual, particles with spherical shapes and homogeneous diameters would be ideal but, as seen in *Figure 1*, such particles did not exist so non-spherical particles without homogeneous diameters were selected, because there were no crystalline silica particles. Silica particles were heat treated at 800°C for 1 h under N_2 atmosphere prior to incorporation. After heat treatment, designated amounts of silica particles were mixed with epoxy resin, degassed under reduced pressure at 120°C for 30 min, followed by addition of a stoichiometric amount of DDM. To prevent the filler from sedimentation, the mixture was precured at 150°C for 10 min. Eventually, the compound was spread into a mould (80 mm × 60 mm × 0.5 mm) and cured at 200°C for 2 h. More detailed descriptions of sample preparation were given in a previous paper[5].

*Studies on mechanical properties of polymer composites by X-ray diffraction IV

†To whom correspondence should be addressed

0032-3861/92/245167-06

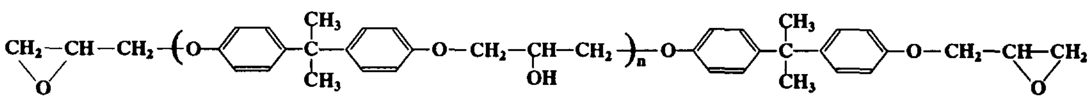

Structure 1

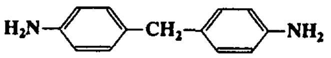

Structure 2

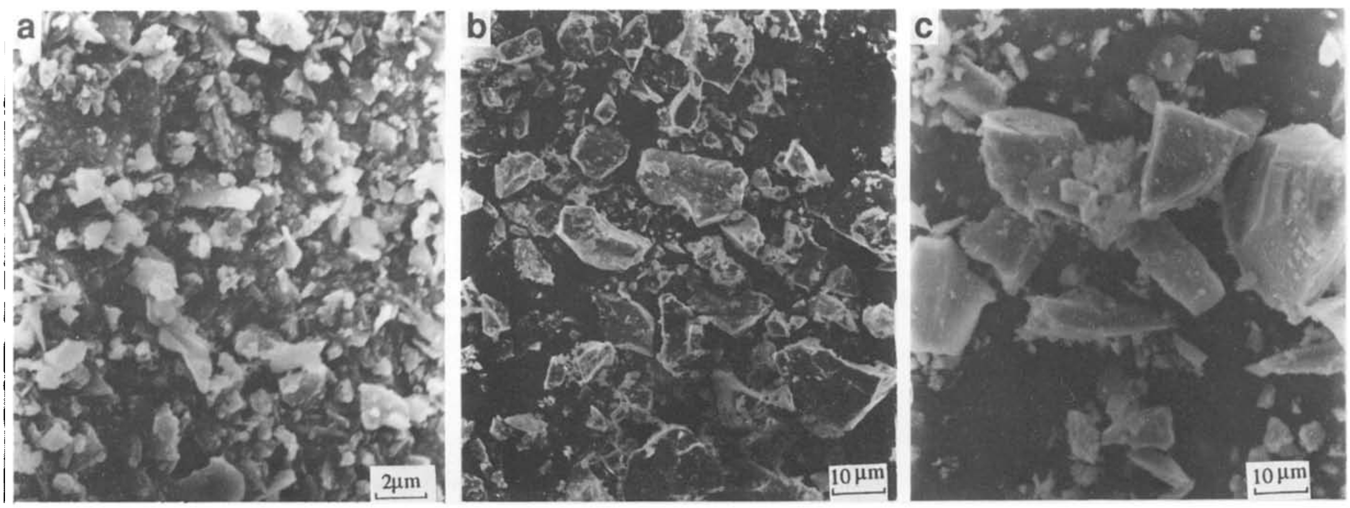

Figure 1 Scanning electron microphotographs of silica particles of various sizes: (a) 1.5 μm; (b) 6.2 μm; (c) 27 μm

The mechanical properties of the specimen were measured by a tensile tester (Shimadzu, Autograph SD-100) at 25°C. The initial length of the specimen was 40 mm and the extension rate was 5 mm min^{-1}.

Measurement of stress on particles by X-ray diffraction

When a tensile stress is applied to a specimen, it is transmitted to the incorporated particles through the matrix. The crystal lattice of the particles is strained by the stress. The crystal strains appear as a shift of diffraction angle 2θ. Consequently, the stress subjected to particles can be evaluated quantitatively by detecting the strain in the crystal by X-ray diffraction. This is the basic principle of the X-ray diffraction method.

A cured specimen was set on an X-ray diffractometer (Rigaku Denki, RAD-B system) operated with $2\theta/\theta$ scan and CuKα radiation. The α-SiO_2 crystal is a hexagonal system ($a=4.913$ Å, $c=5.405$ Å) at 25°C. When symmetrical transmission geometry was used for X-ray diffraction, the (1 0 1) plane of the incorporated silica crystal was employed for the strain measurement, and its diffraction angle was 26.5° for CuKα radiation. With increasing the volume fraction of filler, the absorption coefficient of the specimen became large, and it was difficult to get a sharp peak with sufficient intensity. Thus reflection geometry was also used. In this case, the (3 2 4) plane with a diffraction angle of 152.5° for CuKα1 radiation was employed. Because of its high diffraction angle, the diffraction peak for the (3 2 4) plane was very sensitive to the stress.

The crystal strain ε could be calculated in terms of the relation:

$$\varepsilon=\frac{\Delta d}{d_0} \qquad (1)$$

where d_0 denotes the initial lattice spacing of silica crystal, and Δd is the change in the lattice spacing induced by the constant stress applied. The experimental error in measuring the peak shift was usually evaluated to be less than $\pm 0.003°$ in an angle 2θ which corresponds to about $\pm 0.011\%$ and $\pm 6.4\times10^{-4}\%$ strain for the (1 0 1) and (3 2 4) plane, respectively. Peak positions were determined by a software application; the error in the determination of peak position was less than 0.0001° since the non-linear least-square method was applied in the software application. In order to gain information about the strain distribution in the incorporated particles, strains at different inclination angle, ψ, of the incident X-ray beam were measured[5–7].

Figure 2 is a schematic representation of the measurement of stress on SiO_2 particles in particulate composite by the two kinds of X-ray diffraction methods for reflection geometry and symmetrical transmission geometry. For transmission geometry, the measurement is simple, that is, the observed strain is that in the direction of applied stress. Thus the stress σ_f on particles could be calculated with the following equation:

$$\sigma_f=E_{(101)}\varepsilon \qquad (2)$$

where $E_{(101)}$ is the elastic modulus of the crystal lattice for the (1 0 1) plane of silica (95.9 GPa). This $E_{(101)}$ and

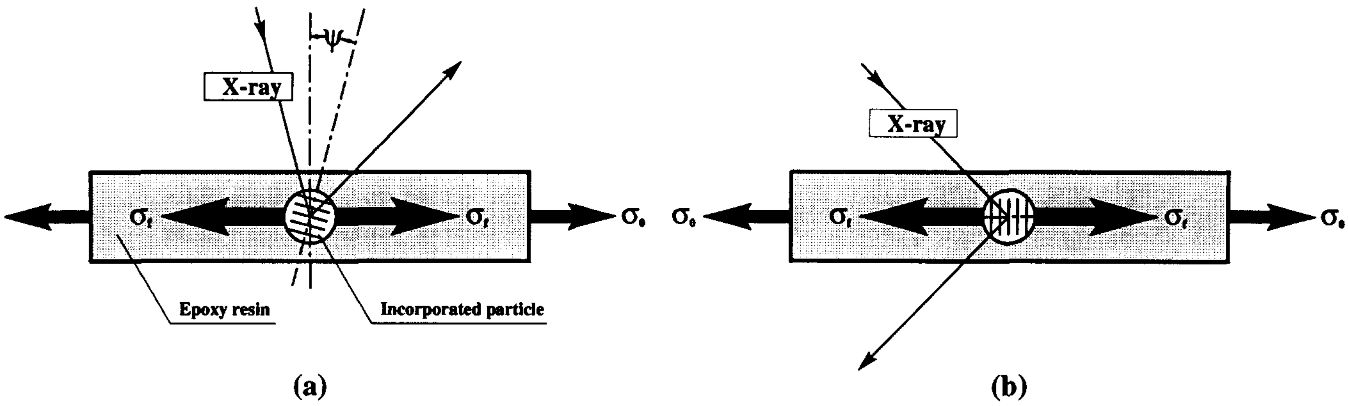

Figure 2 Schematic representation for the measurement of stress on particles by X-ray diffraction: (a) reflection geometry; (b) symmetrical transmission geometry

elastic modulus for other planes are calculated from the experimental values of the elastic stiffness constants[8–12].

On the other hand, for a symmetrical reflection geometry, the observed strain is that in the direction perpendicular to the applied stress σ_0 at $\psi = 0°$, while we can estimate the stress σ_f on particles in the same direction as that of applied stress σ_0 from $\psi = 90°$. Generally, the strain ε_ψ at a given inclination angle can be expressed as:

$$\varepsilon_\psi E_{(324)} = \sigma_f(\sin^2\psi - \nu\cos^2\psi) + P(\cos^2\psi - \nu\sin^2\psi) \quad (3)$$

where $E_{(324)}$ and ν are the elastic modulus (74.5 GPa) and the Poisson ratio (0.33) of crystal lattice for the (3 2 4) plane of silica, respectively. P represents the pressure on the particles in the vertical direction to σ_0. In these cases, shear stress might be brought about in the particles, but its contribution is considered to be negligible. Thus, the principal stress of σ_f and P are discussed here.

Matrix resin deforms much more than the incorporated particles since the Young's modulus of the former is usually much lower than that of the latter. Also, the matrix would contract much more than the incorporated particles in the direction perpendicular to the applied stress. The difference in strains between matrix and particles may cause a pressure P on the particles in the vertical direction to the applied stress.

When strains ε_ψ are measured under various applied stress at $\psi = 0°$, 20°, 30° and 35°, σ_f could be determined by using equation (3) with a non-linear least-squares method.

RESULTS AND DISCUSSION

Figure 3 shows the relationship between applied stress σ_0 and the strain ε_ψ for the (3 2 4) plane of incorporated silica particles (average diameter, 1.5 μm) at various inclination angles ψ for the particulate epoxy composite with a volume fraction of 15.0%. Linear relationships were observed between ε_ψ and σ_0 in every inclination angle ψ, and the strains were always reversible. This indicates that no interfacial destruction takes place up to $\sigma_0 = 30$ MPa. The strain of silica particles showed negative values at $\psi = 0°$. This means that incorporated particles are negatively strained in the direction perpendicular to the applied stress. The strain value increased gradually with increase of the inclination angle ψ, and above $\psi = 25°$, it became positive. From these results, we could estimate the stress to which silica particles were

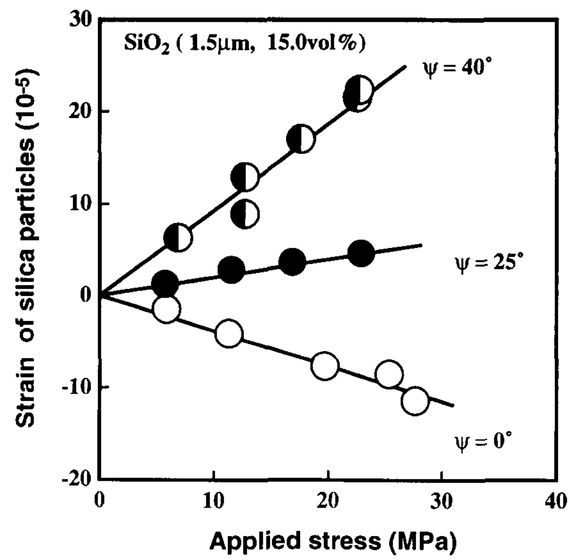

Figure 3 Relationship between strain for the (3 2 4) plane of silica particles at different inclination angle and applied stress for silica particulate composite (average diameter, 1.5 μm, $V_f = 15.0\%$)

subjected using equation (3), with a non-linear least-squares method. Because of the linear relationship between ε_ψ and σ_0, as shown in *Figure 3*, the strain value ε_ψ at a constant applied stress could be determined at every value of ψ.

Figure 4 shows the replot of *Figure 3* for the relationship between strain ε_ψ on particle and $\sin^2\psi$ when σ_0 is 25.0 MPa. ε_ψ increased linearly with $\sin^2\psi$, which coincides with the prediction of equation (3). From the inclination of *Figure 4*, the stress σ_f on silica particles in the direction parallel to the applied stress could be calculated as 56.3 MPa, which is much larger than the applied stress (25 MPa). In other words, the stress on the incorporated particles is about 2.25 times greater than the applied stress (25 MPa). In contrast to this, the matrix resin of the composite would be subjected to less stress than the applied stress, which would result in the reinforcement of the composite. Now the ratio of stress σ_f on particles to applied stress σ_0 is defined as a stress concentration coefficient χ ($= \sigma_f/\sigma_0$). For example, χ is 2.25 for the result of *Figure 4*.

The results shown above were obtained by using

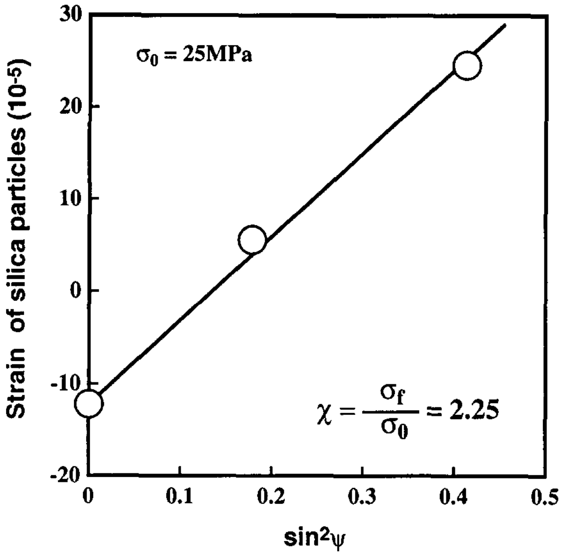

Figure 4 Relationship between strain for the (3 2 4) plane and $\sin^2\psi$ for silica particulate composite

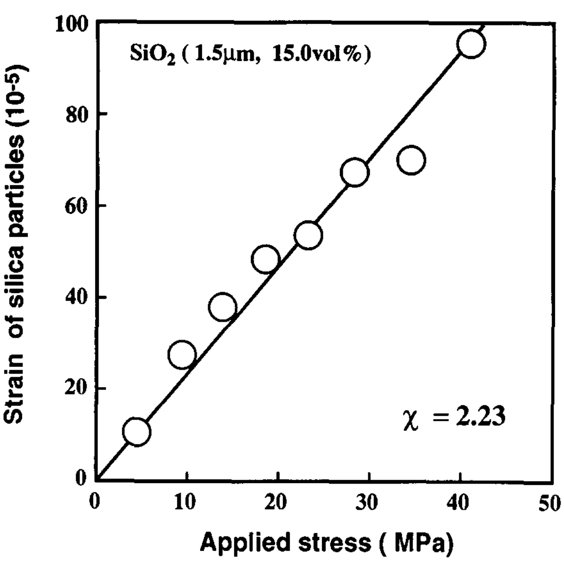

Figure 5 Relationship between strain for the (1 0 1) plane and applied stress of silica particulate composite measured by using the symmetrical transmission geometry

reflection geometry. In order to confirm the validity of this measurement method, ε was measured directly by using transmission geometry.

Figure 5 shows the relationship between applied stress σ_0 and the strain for the (1 0 1) plane of incorporated silica particles (particle diameter 1.5 μm) for the particulate epoxy composite with a volume fraction of filler of 15.0%; this is the same sample used in *Figure 3*. The linear relationship between ε and σ_0 was also obtained by using symmetrical transmission geometry, and no interfacial destruction seems to take place up to $\sigma_0 = 40$ MPa. The stress σ_f on particles could be estimated easily from this curve and the stress concentration coefficient χ was estimated as 2.23, which is almost the same value of χ (2.25) obtained from reflection geometry. For samples with different volume fraction of filler and particle diameter, the χ values from the two types of measurement, that is, reflection and transmission, were confirmed to coincide.

Figure 6 shows the relationship between strain of incorporated silica particles (average diameter of 1.5 μm) and applied stress σ_0 at various inclination angles ψ for specimens with different volume fractions of filler. Strain on particles and applied stress showed a linear relationship in every case. The inclination of these straight lines became lower with increasing volume fraction of filler.

Figure 7 shows the relationship between the χ value and the volume fraction of filler for silica particulate epoxy composite with different particle diameters. χ values were larger than unity in all cases. This indicates that stress was concentrated onto particles and the reinforcement effect appeared up to a volume fraction of filler of 30%, although the χ value decreased with the volume fraction of filler. Comparing the χ value for composites with different particle sizes incorporated, the largest value is for the composite incorporating silica particles of the smallest diameter (1.5 μm) at any volume fraction of filler. Thus the composite material incorporating silica particles of small diameter would be predicted to show high reinforcement properties. Next, we tried to establish relationships between the macroscopic reinforcement effect, increment of macroscopic Young's modulus, stress concentration coefficient χ and the volume fraction of filler.

Particles incorporated in the composite material were subjected to a larger stress σ_f than the average stress σ_0 as shown above, and the matrix was considered to be subjected to smaller stress. By using the χ value, the average stress σ_m in the matrix can be expressed as follows:

$$\sigma_m = \sigma_0 \frac{1-\chi V_f}{1-V_f} \quad (4)$$

where V_f represents the volume fraction of incorporated particles.

The strain of the matrix is restricted by the presence of the particles. When strain distribution interposed between two particles is assumed to be that shown schematically in *Figure 8*, the strain $\varepsilon(l)$ at a position l $(-L_0/2 \leqslant l \leqslant +L_0/2)$ can be expressed by the following equation:

$$\varepsilon(l) = \varepsilon_{min} + (\varepsilon_{max} - \varepsilon_{min})\left[1 - \exp\left(\frac{L_0 - 2l}{2\delta}\right) - \exp\left(-\frac{L_0 + 2l}{2\delta}\right)\right]\left(-\frac{L_0}{2} \leqslant l \leqslant \frac{L_0}{2}\right) \quad (5)$$

where ε_{min} is the strain of matrix at the particle surface, $\varepsilon_{min} = \chi\sigma_0/E_f$, ε_{max} is the strain of the matrix with no restriction from particles, $\varepsilon_{max} = \sigma_m/E_m$, L_0 is the average distance between particle surfaces, $L_0 = \{(\pi/6)[(1 - V_f)/V_f]\}^{1/3}d$, where d is the average diameter of particles (1.5 μm, 6.2 μm or 27 μm). δ is a position where $\varepsilon_{max} - \varepsilon(l) = \{\varepsilon_{max} - \varepsilon_{min}\}/e$ (see *Figure 8*), and its experimental value is 1.5 μm for the system studied.

The average strain ε_{av} for the matrix could be calculated from the following equation by integrating $\varepsilon(l)$:

$$\varepsilon_{av} = \left(\frac{1}{L_0}\right)\int_{-L_0/2}^{L_0/2} \varepsilon(l)dl \quad (6)$$

With the average strain value ε_{av}, the macroscopic Young's modulus E_c of the whole composite material

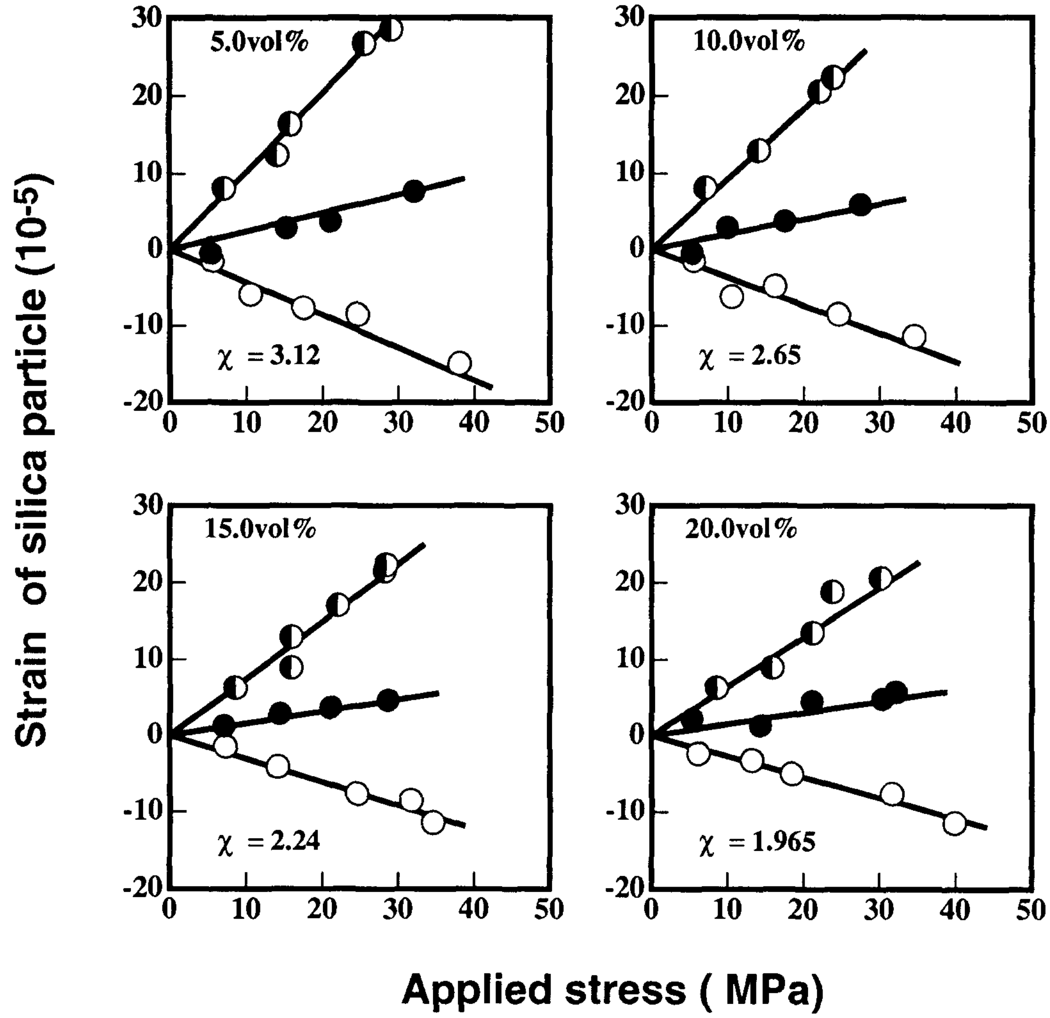

Figure 6 Relationship between strain for the (3 2 4) plane of silica particles at different inclination angle, ψ(◐, 40°; ●, 25°; ○, 0°) and applied stress for silica particulate composite with various volume fractions of filler

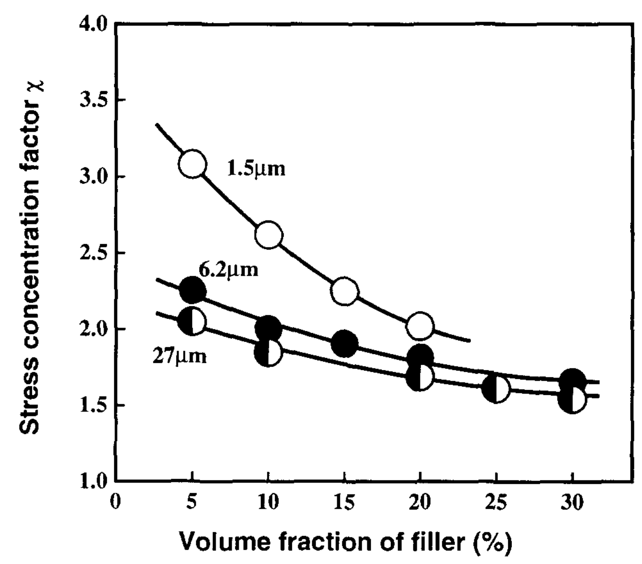

Figure 7 Relationship between the stress concentration factor χ and the volume fraction of filler for silica particulate epoxy composite

could be calculated from the following equation:

$$\frac{1}{E_c}=\frac{\chi}{E_f}+\left(\frac{1-\chi V_f}{(1-V_f)E_m}-\frac{\chi}{E_f}\right)\left\{1-\frac{2\delta}{L_0}\left[1-\exp\left(-\frac{L_0}{\delta}\right)\right]\right\} \quad (7)$$

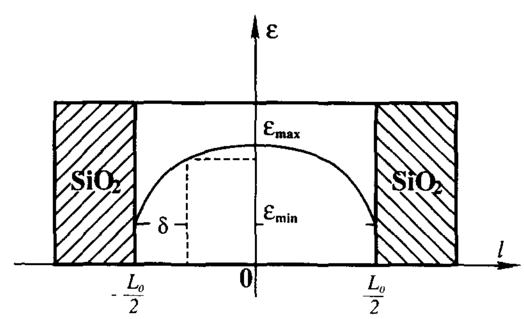

Figure 8 Schematic representation for the strain distribution of the matrix interposed between silica particles in particulate composite material

For large particles, the restriction of strain of the matrix by particles could be neglected, and equation (7) could be simplified into the following equation at a low volume fraction:

$$E_c=\frac{1-V_f}{1-\chi V_f}E_m \quad (8)$$

Figure 9 shows the relationship between volume fraction of filler and the macroscopic Young's modulus E_c of silica particulate composite. The solid lines indicate the calculated result of equation (7). Prediction from Kerner's equation[3] is also superposed on the figure as a

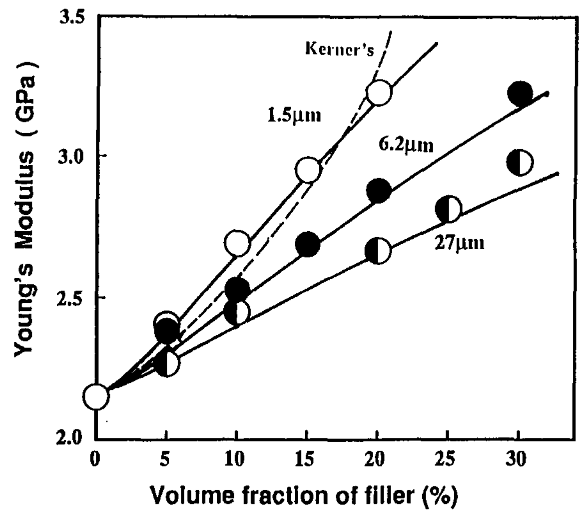

Figure 9 Relationship between Young's modulus and the volume fraction of filler for silica particulate epoxy composite

broken line. E_c increased with the incorporation of filler and this tendency was enhanced for particles of smaller diameter. Results from Kerner's equation fit only for the composite incorporated with silica particles of 1.5 μm. However, the calculated value from equation (7) agreed well with the experimental values. Accordingly, the increment of the macroscopic modulus could be expressed quantitatively by considering the stress concentration onto particles. The restriction of the deformation of matrix by the incorporation of particles is concluded to bring the reinforcement effect to the composite. Comparing the macroscopic Young's modulus of composite with the same volume fraction of fillers, the reinforcement effect increased with decreasing particle sizes, because the distance between the interfaces of particles decreased with the decrease of particle sizes. This is the main reason why smaller particles are much more effective for the reinforcement of epoxy resin.

CONCLUSION

The stress on particles in silica particulate epoxy composites under constant load was measured by the X-ray diffraction method. The stress on particles was found to be several times larger than the applied stress. This indicates that the stress was concentrated onto incorporated particles, which is considered to bring about mechanical reinforcement of the composite. The ratio of the stress on particles to the applied stress, χ, decreased with the filler size and the increase in volume fraction of filler. By using the χ value, an increment of macroscopic Young's modulus with the incorporation of filler could be explained quantitatively.

ACKNOWLEDGEMENT

The authors are grateful to Tatsumori Co. for supplying the air blown fractionated silica particles.

REFERENCES

1 Nielsen, L. E. 'Mechanical Properties of Polymer and Composites', Marcel Dekker, New York, 1975
2 Ahmed, S. and Jones, F. R. *J. Mater. Sci.* 1990, **25**, 4933
3 Nakamae, K., Nishino, T., Xu, A.-R., Matsumoto, T. and Miyamoto, T. *J. Appl. Polym. Sci.* 1990, **40**, 2231
4 Nishino, T., Xu, A.-R., Matsumoto, T., Matsumoto, K. and Nakamae, K. *J. Appl. Polym. Sci.* 1992, **45**, 1239
5 Nakamae, K., Nishino, T. and Xu, A.-R. *Polymer* 1992, **33**, 2720
6 Cheskis, H. P. and Heckel, R. W. *Met. Trans.* 1970, **1**, 1931
7 Cullity, B. D. 'Elements of X-ray Diffraction', 2nd Edn, Addison-Wesley, Reading, 1980, Ch. 16
8 Mason, W. P. (Ed.) 'Physical Acoustics' Vol. 3B, Academic Press, New York, 1965
9 Bigg, D. M. *Polym. Eng. Sci.* 1976, **16**, 725
10 Black, W. B. *J. Macromol. Sci., Chem.* 1973, **7**, 3
11 Morgan, P. W. *et al. Macromolecules* 1977, **10**, 1381
12 McCullough, R. L., Wu, C. T., Seferis, J. C. and Lindenmeyer, P. H. *Polym. Eng. Sci.* 1976, **16**, 371
13 Kerner, E. H. *Proc. Phys. Soc.* 1956, **69B**, 808